Biaxial Flexural Strength of 3D-Printed Splint Materials

Johann Wulff , Angelika Rauch , Michael Schmidt , Martin Rosentritt *

Posted Date: 23 August 2023

doi: 10.20944/preprints202308.1631.v1

Keywords: 3D-printing; oral splint; biaxial flexural strength; TMD; PMMA; DLP

Article

Biaxial Flexural Strength of 3D-Printed Splint Materials

Johann Wulff, Angelika Rauch, Michael Schmidt, and Martin Rosentritt *

Department of Prosthetic Dentistry, UKR University Hospital Regensburg, 93042 Regensburg, Germany
* Correspondence: martin.rosentritt@ukr.de; +49-941-944-6054

Abstract: Printed oral splints are a therapeutic alternative in the treatment of functional disorders. Their mechanical properties are crucial to their clinical success and their performance can vary depending on cleaning, post-polymerization, or build orientation. This in vitro study aimed to compare the biaxial flexural strength of the chosen materials depending on the aforementioned parameters. 720 discs (n = 15 per group, 16 mm x 2 mm) were printed from splint materials. Printing was performed under 90°, 45°, or 0° orientation to the building platform with supporting structures. Specimens were either automatically or manually cleaned with isopropanol. Post-polymerization was performed with LED- or Xenon-light. Biaxial flexural strength (BFS) was determined with a piston-on-3-ball test after 24 hours or 60 days water storage (37°C). Test specimens were preloaded with 0.5 N and the load was applied by a piston of 1.6 mm in diameter at 1 mm/min crosshead speed. Statistics were performed by using descriptive statistics, ANOVA, and Levene-tests. Mean BFS after 24 hours of storage varied between 79 MPa and 157 MPa. After 60 hours the BFS significantly decreased and revealed values ranging from 72-127 MPa ($mean_{24}$ 113 MPa, $mean_{60}$ 97 MPa; $p<0.001$). No significant differences could be determined between the materials ($p=0.103$) or between the different cleaning procedures ($p=0.321$). Post-polymerization yielded higher means with LED- (P1: 115 MPa) than with Xenon-light (P2: 95 MPa; $p<0.001$). Regarding position, the mean values ranged from 101 MPa for 0°, 102 MPa for 45°, and 115 MPa for 90°, which was significantly different ($p<0.001$). Build orientation of 90° and post-polymerization with LED-light provided significantly higher biaxial flexural strength and should be used to guarantee optimal strength of splint materials. Aging decreased the biaxial flexural strength of the tested specimens.

Keywords: 3D-printing, oral splint, biaxial flexural strength, TMD, PMMA, DLP

1. Introduction

Oral splints are frequently used for the treatment of temporomandibular disorders (TMD) and parafunctions such as bruxism [1]. Cast methacrylates or deep-drawn thermoplastics are typically utilized to build adjusted oral splints [2]. However, additive manufacturing (AM; 3D-printing) is a viable alternative to producing splints more quickly in case of fracture or loss. Liquid photopolymer resins are used in the digital light processing (DLP) VAT 3D-printing systems [3,4]. Alharbi et al. (2016) stated that in order to optimize the process, materials and printing techniques must be coordinated [5]. This can be done, for instance, by matching the kind and speed of the printer with the proper viscosity of the utilized resin [6]. The splints must be washed with solvent (such as 2-Propanol) directly after printing in order to get rid of any uncured monomer [7]. Although conversion is partially limited [8,9], AM enables the fabrication of splints with adequate accuracy [10–12]. To guarantee adequate final polymerization, the splints are post-polymerized using external light curing devices that use LED- or Xenon-light after cleaning. Each printing technique differs significantly from the other; thus, the impacts of the material, cleaning, and polymerization are particularly relevant.

According to Park et al., printed splints are more flexible than hand-cast or milled systems while maintaining adequate mechanical strength [13]. The mechanical properties of the splints appear to be influenced by the thickness and orientation of the individual layers during manufacturing [14–17]. Layer orientation within the object must be taken into account, as it affects the strength of the material [5,18].

 doi:10.20944/preprints202308.1631.v1

The mechanical properties of the splint materials are to be taken into consideration when designing an object. Incorrect design or low strength can lead to deformation, fracture or reduced performance of the splint. As bite forces yield values up to 999.3 N and as a high frequency for insertion and removal of splints is common during clinical service, the flexural strength of splint materials is of great importance [19–22]. Tests such as the three-point bending test and the biaxial flexural strength test can be used to verify if materials meet the requirements, providing relevant threshold values for the resins [23](DIN EN ISO 20795-1:2013-06). An advantage of the biaxial test over a standard three-point bend test is that edge effects are avoided. The uniformity of the stress field can be ensured over a large area of the specimen, and the influence of specimen orientation (expressed, for example, with the printing orientation) can be eliminated. Movable supports or additional intermediate soft layers on the surfaces of the specimens eliminate frictional effects. Long-term effects, such as those brought on by a damp environment, should be taken into account in order to imitate clinical performance.

The hypothesis of this in vitro study was that build orientation has no effect on the biaxial flexural strength of different 3D printed splint materials independent of post-polymerization, washing, or storage.

2. Materials and Methods

Specimens (diameter: 16 mm; height: 2 mm) from two splint materials (M1: Luxaprint OrthoPlus, DMG, Hamburg, Germany; M2: V-Print Splint, VOCO, Cuxhaven, Germany) were fabricated with a P30+ DLP-printer (Straumann, Basel, Switzerland). Printing was performed under 90°, 45°, or 0° orientation to the building platform in 100 µm layers with supporting structures. Specimens were either automatically (AUTO: Straumann P Wash, Straumann) or manually cleaned (MAN: VOCO Pre-/Main-Clean protocol, VOCO) with isopropanol. Post-polymerization was performed with LED- (LED: Cure, Straumann) or Xenon-light (XEN: Otoflash N171, Ernst Hinrichs Dental, Goslar, Germany). In total 720 specimens – 15 for each group and test – were printed. The supporting structures were removed, the specimens were ground to the final dimensions with silicon carbide paper grit P600/1200 (Paper SiC P600/1200; Struers GmbH, Willich, Germany), pre-polished with pumice stone powder, and finally high-gloss polished (Universal Polishing Paste; Ivoclar Vivadent, Schaan, Liechtenstein). Afterwards, the specimens were cleaned in an ultrasonic bath for two minutes to remove any excess material, rinsed with distilled water, and dried with compressed air. Specimens were stored in distilled water at 37°C for either 24 hours (n = 360) or 60 days (n = 360).

Table 1. Study design, materials and devices.

			Manufacturer/LOT
Printer		P30+ (digital light processing)	Straumann, Basel, Switzerland
Orientation	**0°**		
	45°		
	90°		
Cleaning	**AUTO**	P Wash (isopropanol): pre-cleaning 3:10 min, cleaning 2:20 min, drying 1:30 min	Straumann, Basel, Switzerland
	MAN	Pre-/Main-Clean (isopropanol): pre-cleaning 3:00 min, ultrasonic: 2:00 min, air-drying: 1:00 min	VOCO, Cuxhaven, Germany
	LED	P Cure:	Straumann,

Post polymerization		LED, 10 min, vacuum, UV–A: 400 - 315 nm; UV-B 315 - 280 nm, heating	Basel, Switzerland
	XEN	Otoflash G171: 2 x 2000 Xenon flashes, 280-700 nm, maximum between 400 - 500 nm	NK-OPTIK, Baierbrunn, Germany
Materials	**M1**	Luxaprint OrthoPlus: > 90% bisphenol A dimethacrylate, 385/405 nm, flexural strength ≥ 70 MPa, flexural modulus ≥ 1 GPa, Shore D ≥ 60	DMG, Hamburg, Germany/LOT 218479
	M2	V-Print Splint: acrylate, Bis-EMA, TEGDMA, hydroxypropyl methacrylate, butylated hydroxytoluene, diphenyl(2,4,6-trimethylbenzoyl) phosphine oxide, 385 nm, flexural strength 75 MPa, flexural modulus ≥ 2.1 GPa, water uptake 27.7 µg/mm³, solubility < 0.1 µg/mm³	VOCO, Cuxhaven, Germany/LOT 2023138

Biaxial flexural strength (BFS) was determined with a piston-on-three-ball test according to ISO 6872 (universal testing machine Z2.0, Zwick/Roell, Ulm, Germany; THS1620, Grip-Engineering Thümler, Nürnberg, Germany). Specimens were positioned on a supporting ring-like bearing that consisted of three stainless steel spheres (diameter: 3 mm), which were arranged in the form of an equilateral triangle at 120° (diameter: 10 mm). Specimens were placed centrally on the bearing. A polyethylene film (thickness: 0.05 mm, 1-7090, neoLab Migge, Heidelberg, Germany) was placed between the specimen and the piston as well as between the specimen and the bearing in order to evenly distribute the contact force. Specimens were preloaded with 0.5 N. The piston (diameter: 1.6 mm) applied the load at 1 mm/min.

The fracture force was measured and the biaxial flexural strength was calculated according to the following equation:

$$\sigma = -0.2387P(X-Y) / d^2 \quad (1)$$

Legend:
σ = biaxial flexural strength (MPa);
P = fracture force (N);
d = specimen thickness at fracture origin (mm).
The variables X and Y were determined as follows:

$$X = (1+v) \ln(r_2/r_3)^2 + [(1-v)/2] r_2^2/r_3 \quad (2)$$

$$Y = (1+v) [1+\ln(r_1/r_3)^2] + (1-v) (r_1/r_3)^2 \quad (3)$$

Legend:
v = Poisson's ratio (0.3) [24];
r_1 = radius of the supporting bearing;
r_2 = radius of the loaded area;
r_3 = radius of the specimen.

Statistics were performed (SPSS 26.0, IBM, Armonk, NY, USA) for computing descriptive statistics and to analyse differences between mean values with a one-way ANOVA with a significance level of α <0.05. Intermediate subject effects were calculated.

3. Results

Preprints (www.preprints.org) | NOT PEER-REVIEWED | Posted: 23 August 2023 doi:10.20944/preprints202308.1631.v1

The mean BFS after 24 hours of storage varied between 78 MPa and 158 MPa. After 60 hours, the BFS revealed values ranging from 71 MPa to 128 MPa (Table 2, Fig 1). A significant influence of aging could be observed ($mean_{24}$ 113 MPa, $mean_{60}$ 97 MPa; $p<0.001$). No significant differences could be determined between the materials ($p=0.103$) or between the different cleaning procedures ($p=0.321$). Post-polymerization had a significant influence on BFS ($p<0.001$), while LED revealed higher means (115 MPa) than Xenon (95 MPa). Regarding orientation, the mean values ranged between 101 MPa for 0°, 102 MPa for 45°, and 115 MPa for 90°, which was significantly different (one-way ANOVA: df: 47; F: 26.190; $p<0.001$).

Table 2. Biaxial flexural strength (BFS in MPa, mean, standard deviation [SD]) of the materials after different orientation to the building platform, cleaning, post-polymerization, and storage time in water.

Orientation to building platform	Material	Cleaning	Post-polymerization	storage time (water 37°C)	BAF	
					mean	SD
90°	M1	C1	P1	24 h	125.2	5.3
				60 d	119.7	7.5
			P2	24 h	119.3	12.8
				60 d	112.8	12.6
		C2	P1	24 h	121.3	14.9
				60 d	106.9	14.2
			P2	24 h	83.3	6.9
				60 d	82.8	8.3
	M2	C1	P1	24 h	157.5	16.2
				60 d	127.1	6.9
			P2	24 h	122.1	11.6
				60 d	89.5	7.5
		C2	P1	24 h	145.8	11.5
				60 d	120.3	11.9
			P2	24 h	127.9	8.0
				60 d	89.8	5.8
45°	M1	C1	P1	24 h	109.6	28.8
				60 d	101.7	15.3
			P2	24 h	95.1	10.1
				60 d	83.0	9.6
		C2	P1	24 h	122.2	20.4
				60 d	116.5	14.6
			P2	24 h	100.6	14.8
				60 d	90.7	13.3
	M2	C1	P1	24 h	111.1	17.3
				60 d	95.3	17.8
			P2	24 h	104.2	13.8
				60 d	78.6	12.5
		C2	P1	24 h	106.5	23.9
				60 d	84.4	17.0

Preprints (www.preprints.org) | NOT PEER-REVIEWED | Posted: 23 August 2023 doi:10.20944/preprints202308.1631.v1

			P2	24 h	101.4	15.2
				60 d	72.7	15.4
0°	M1	C1	P1	24 h	105.4	16.9
				60 d	107.4	9.1
			P2	24 h	91.1	15.0
				60 d	95.5	6.9
		C2	P1	24 h	116.7	12.1
				60 d	109.6	15.4
			P2	24 h	98.5	6.4
				60 d	91.3	5.1
	M2	C1	P1	24 h	119.4	25.9
				60 d	93.2	24.8
			P2	24 h	78.6	11.1
				60 d	71.9	13.5
		C2	P1	24 h	141.3	9.3
				60 d	102.9	13.0
			P2	24 h	115.2	14.9
				60 d	90.9	11.7

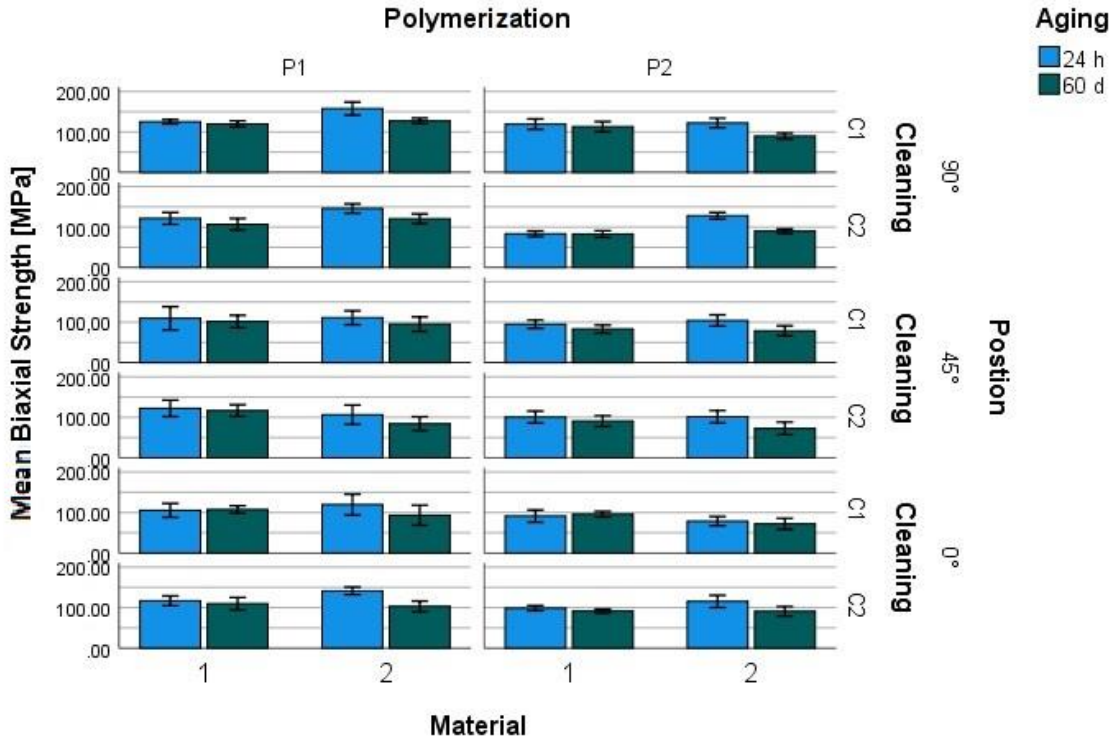

Figure 1. Mean biaxial flexural strength of splint materials (M) depending on polymerization (P), cleaning (C), storage in –water (37°C) and printing orientation to the building platform.

The Levene-test revealed that the error variance of the dependent variable was different across groups ($p<0.001$), thus a significance level of 0.01 was set. Intermediate subject effects were determined for the combination of material and position/aging ($p<0.001$), position and

Preprints (www.preprints.org) | NOT PEER-REVIEWED | Posted: 23 August 2023 doi:10.20944/preprints202308.1631.v1

cleaning/polymerization (p<0.001), material and position and cleaning (p<0.001), material and position and polymerization (p<0.001), material and cleaning and polymerization (p<0.001). All other combinations revealed no intermediate effects (p≥0.012) (Table 3).

Table 3. Intermediate subject effects (significance, α=0.01, R^2 = .647, grey: significant effects).

	F	p-Value
material	2.668	.103
orientation	100,342	<.001
cleaning	.984	.321
polymerization	356.934	<.001
aging	228.539	<.001
material * position	36.020	<.001
material * cleaning	8.985	0.003
material * polymerization	2.966	0.085
material * aging	92.072	<.001
position * cleaning	46.331	<.001
position * polymerization	6.678	.001
position * aging	2.904	.056
cleaning * polymerization	.542	.462
cleaning * aging	5.412	.020
polymerization * aging	.124	.724
material * position * cleaning	28.301	<.001
material * position * polymerization	10.567	<.001
material * position * aging	2.274	.104
material * cleaning * polymerization	25.823	<.001
material * cleaning * aging	.650	.420
material * polymerization * aging	.026	.872
position * cleaning * polymerization	1.688	.186
position * cleaning * aging	3.345	.036
position * polymerization * aging	4.367	.013
cleaning * polymerization * aging	.000	.988
material * position * cleaning * polymerization	3.557	.029
material * position * cleaning * aging	.318	.727
material * position * polymerization * aging	4.161	.016
material * cleaning * polymerization * aging	.945	.331
position * cleaning * polymerization * aging	.222	.801
material * position * cleaning * polymerization * aging	1.055	.349

4. Discussion

The hypothesis of this in vitro study that build orientation has no effect on the BFS of 3D printed splint materials independent on post-polymerization, washing, or storage could not be confirmed. Build orientation had a significant effect on the BFS, as did the type of polymerization and storage.

Even though a lot of literature is available on 3D-printed dental products' accuracy, there is limited evidence to their mechanical properties. Earlier studies have compared 3D-printed to milled

 doi:10.20944/preprints202308.1631.v1

and pressed splint materials that showed 3D-printed resins had lower flexural strength and hardness values after aging [3]. This might be caused by increased water sorption.

The highest BFS values were obtained from samples printed at 90°. Whereas a reduction in flexural strength was found while implementing a reduced printing angle. Previous investigations on build orientation with AM resins revealed that the mechanical properties of printed materials are affected by the orientation of the individual layers during printing [14,15]. An anisotropy of additive materials caused by the printing orientation was previously described [25,26]. While using DLP, the UV-light is projected over an assembly of numerous micro-mirrors, resulting in a simultaneously polymerized layer consisting of a multitude of voxels. In the vertical direction, the voxels are polymerized without gaps forming columns layer by layer. However, in the lateral direction, the voxels are separated from each other by thin interstitial or shadow areas yielding a reduced degree of polymerization. These areas correspond to the boundaries of each micro-mirror, which may represent a potential weakness [25,27,28]. The conversion in these areas takes place first during the post curing phase [25].

The type of cleaning procedure used seemed to have no significant effect on the flexural strength of the tested 3D-printed materials. Xu et al. observed a decrease in the flexural strength of materials when significantly increasing the cleaning time from 5 minutes to 12 hours [29]. Significant effects of the utilized cleaning procedure could be observed while testing other properties of splint materials, e.g., cytotoxicity. This research showed a decrease in cytotoxicity while using automatic instead of manual cleaning of the specimens [30].

In the current investigation, post-curing with LED-light resulted in higher biaxial flexural strength values. This might be attributed to a higher conversion of double bonds or a reduced number of residual monomers. The reasons for higher conversion might be a different energy input or the applied light wavelength from the polymerization devices adapting to the absorption spectrum of the photo initiator. With the utilized parameters, Xenon polymerization seems to be less effective and consistent than LED-curing. This observation is corroborated by a previous investigation, which observed that vacuum curing and the heating function of LED-light can increase the conversion of the specimens and reduce oxygen inhibition on the outermost layers [31]. The chain polymerization of methacrylate resins is a complex reaction that depends, e.g., on the composition of the material, the curing devices, and environmental conditions [32]. The degree of conversion, hardness, and biocompatibility of resins used in 3D-printing are all increased by a longer post-polymerization [33,34]. The effective combination of heat and light during the post-polymerization can also increase the degree of conversion [9].

Water storage had a crucial effect on BFS by reducing mean values between 1% and 30%. The decrease in mean BFS after aging might be attributed to significant water uptake (-27.7 µg/mm3) or solubility (<0.1 µg/mm3). Various research groups have already determined that the behavior of dental resins is affected by the corrosive influence of water and/or by cyclic masticatory forces. These can cause degradation, elution, relaxation, swelling, or visco-elastic effects, accelerated crack growth, and reduced wear resistance [22,35–37].

5. Conclusions

Specimens printed at a build angle of 90° showed the highest biaxial flexural strength values. Specimens cured with an LED device showed higher biaxial strength values than those cured with Xenon-light. The aging of the specimens significantly decreased the mechanical properties of the materials.

Therefore, post-processing of 3D-printed restorations should be carefully matched in order to achieve the best results regarding their mechanical properties in terms of biaxial strength.

Author Contributions: J.W. investigation, data collection, writing – original draft preparation, writing – review and editing; A.R. data curation, writing – review and editing; M.S. writing – review and editing; M.R. investigation, data curation, writing – original draft preparation, supervision. All authors have read and agreed to the published version of the manuscript.

Funding: This research received no external funding.

Institutional Review Board Statement: Not applicable

Conflicts of Interest: The authors declare that they have no known competing financial interests or personal relationships that could have appeared to influence the work reported in this paper.

References

1. Lobbezoo, F.; Ahlberg, J.; Raphael, K.G.; Wetselaar, P.; Glaros, A.G.; Kato, T.; Santiago, V.; Winocur, E.; Laat, A. de; Leeuw, R. de; et al. International consensus on the assessment of bruxism: Report of a work in progress. *J. Oral Rehabil.* **2018**, *45*, 837–844, doi:10.1111/joor.12663.
2. Lutz, A.-M.; Hampe, R.; Roos, M.; Lümkemann, N.; Eichberger, M.; Stawarczyk, B. Fracture resistance and 2-body wear of 3-dimensional-printed occlusal devices. *J. Prosthet. Dent.* **2019**, *121*, 166–172, doi:10.1016/j.prosdent.2018.04.007.
3. Berli, C.; Thieringer, F.M.; Sharma, N.; Müller, J.A.; Dedem, P.; Fischer, J.; Rohr, N. Comparing the mechanical properties of pressed, milled, and 3D-printed resins for occlusal devices. *J. Prosthet. Dent.* **2020**, doi:10.1016/j.prosdent.2019.10.024.
4. Dedem, P.; Türp, J.C. Digital Michigan splint - from intraoral scanning to plasterless manufacturing. *Int. J. Comput. Dent.* **2016**, *19*, 63–76.
5. Alharbi, N.; Osman, R.; Wismeijer, D. Effects of build direction on the mechanical properties of 3D-printed complete coverage interim dental restorations. *J. Prosthet. Dent.* **2016**, *115*, 760–767, doi:10.1016/j.prosdent.2015.12.002.
6. Kessler, A.; Reymus, M.; Hickel, R.; Kunzelmann, K.-H. Three-body wear of 3D printed temporary materials. *Dent. Mater.* **2019**, *35*, 1805–1812, doi:10.1016/j.dental.2019.10.005.
7. Wedekind, L.; Güth, J.-F.; Schweiger, J.; Kollmuss, M.; Reichl, F.-X.; Edelhoff, D.; Högg, C. Elution behavior of a 3D-printed, milled and conventional resin-based occlusal splint material. *Dent. Mater.* **2021**, *37*, 701–710, doi:10.1016/j.dental.2021.01.024.
8. Alifui-Segbaya, F.; Bowman, J.; White, A.R.; George, R.; Fidan, I. Characterization of the Double Bond Conversion of Acrylic Resins for 3D Printing of Dental Prostheses. *Compend. Contin. Educ. Dent.* **2019**, *40*, e7-e11.
9. Perea-Lowery, L.; Gibreel, M.; Vallittu, P.K.; Lassila, L. Evaluation of the mechanical properties and degree of conversion of 3D printed splint material. *J. Mech. Behav. Biomed. Mater.* **2021**, *115*, 104254, doi:10.1016/j.jmbbm.2020.104254.
10. Nestler, N.; Wesemann, C.; Spies, B.C.; Beuer, F.; Bumann, A. Dimensional accuracy of extrusion- and photopolymerization-based 3D printers: In vitro study comparing printed casts. *J. Prosthet. Dent.* **2020**, doi:10.1016/j.prosdent.2019.11.011.
11. Park, G.-S.; Kim, S.-K.; Heo, S.-J.; Koak, J.-Y.; Seo, D.-G. Effects of Printing Parameters on the Fit of Implant-Supported 3D Printing Resin Prosthetics. *Materials (Basel)* **2019**, *12*, doi:10.3390/ma12162533.
12. Reymus, M.; Fabritius, R.; Keßler, A.; Hickel, R.; Edelhoff, D.; Stawarczyk, B. Fracture load of 3D-printed fixed dental prostheses compared with milled and conventionally fabricated ones: the impact of resin material, build direction, post-curing, and artificial aging-an in vitro study. *Clin. Oral Investig.* **2020**, *24*, 701–710, doi:10.1007/s00784-019-02952-7.
13. Park, S.-M.; Park, J.-M.; Kim, S.-K.; Heo, S.-J.; Koak, J.-Y. Flexural Strength of 3D-Printing Resin Materials for Provisional Fixed Dental Prostheses. *Materials (Basel)* **2020**, *13*, 3970, doi:10.3390/ma13183970.
14. Nold, J.; Wesemann, C.; Rieg, L.; Binder, L.; Witkowski, S.; Spies, B.C.; Kohal, R.J. Does Printing Orientation Matter? In-Vitro Fracture Strength of Temporary Fixed Dental Prostheses after a 1-Year Simulation in the Artificial Mouth. *Materials (Basel)* **2021**, *14*, 259, doi:10.3390/ma14020259.
15. Hada, T.; Kanazawa, M.; Iwaki, M.; Arakida, T.; Soeda, Y.; Katheng, A.; Otake, R.; Minakuchi, S. Effect of Printing Direction on the Accuracy of 3D-Printed Dentures Using Stereolithography Technology. *Materials (Basel)* **2020**, *13*, 3405, doi:10.3390/ma13153405.
16. Marcel, R.; Reinhard, H.; Andreas, K. Accuracy of CAD/CAM-fabricated bite splints: milling vs 3D printing. *Clin. Oral Investig.* **2020**, *24*, 4607–4615, doi:10.1007/s00784-020-03329-x.
17. Grymak, A.; Aarts, J.M.; Ma, S.; Waddell, J.N.; Choi, J.J.E. Comparison of hardness and polishability of various occlusal splint materials. *J. Mech. Behav. Biomed. Mater.* **2021**, *115*, 104270, doi:10.1016/j.jmbbm.2020.104270.
18. Puebla, K.; Arcaute, K.; Quintana, R.; Wicker, R.B. Effects of environmental conditions, aging, and build orientations on the mechanical properties of ASTM type I specimens manufactured via stereolithography. *Rapid Prototyping Journal* **2012**, *18*, 374–388, doi:10.1108/13552541211250373.
19. Calderon, P.d.S.; Kogawa, E.M.; Lauris, J.R.P.; Conti, P.C.R. The influence of gender and bruxism on the human maximum bite force. *J. Appl. Oral Sci.* **2006**, *14*, 448–453, doi:10.1590/s1678-77572006000600011.
20. Nishigawa, K.; Bando, E.; Nakano, M. Quantitative study of bite force during sleep associated bruxism. *J. Oral Rehabil.* **2001**, *28*, 485–491, doi:10.1046/j.1365-2842.2001.00692.x.
21. Hickl, V.; Strasser, T.; Schmid, A.; Rosentritt, M. Pull-off behavior of hand-cast, thermoformed, milled and 3D printed splints. *Int. J. Prosthodont.* **2022**, doi:10.11607/ijp.8068.

22. Rosentritt, M.; Behr, M.; Strasser, T.; Schmid, A. Pilot in-vitro study on insertion/removal performance of hand-cast, milled and 3D printed splints. *J. Mech. Behav. Biomed. Mater.* **2021**, *121*, 104612, doi:10.1016/j.jmbbm.2021.104612.
23. *DIN EN ISO 20795-1:2013-06, Zahnheilkunde_- Kunststoffe_- Teil_1: Prothesenkunststoffe (ISO_20795-1:2013); Deutsche Fassung EN_ISO_20795-1:2013;* Beuth Verlag GmbH: Berlin.
24. Lee, H.; Wang, J.; Park, S.-M.; Hong, S.; Kim, N. Analysis of excessive deformation behavior of a PMMA-touch screen panel laminated material in a high temperature condition. *Korea-Aust. Rheol. J.* **2011**, *23*, 195–204, doi:10.1007/s13367-011-0024-4.
25. Dizon, J.R.C.; Espera, A.H.; Chen, Q.; Advincula, R.C. Mechanical characterization of 3D-printed polymers. *Additive Manufacturing* **2018**, *20*, 44–67, doi:10.1016/j.addma.2017.12.002.
26. Zohdi, N.; Yang, R.C. Material Anisotropy in Additively Manufactured Polymers and Polymer Composites: A Review. *Polymers* **2021**, *13*, doi:10.3390/polym13193368.
27. Monzón, M.; Ortega, Z.; Hernández, A.; Paz, R.; Ortega, F. Anisotropy of Photopolymer Parts Made by Digital Light Processing. *Materials (Basel)* **2017**, *10*, doi:10.3390/ma10010064.
28. Garcia, J.; Yang, Z.; Mongrain, R.; Leask, R.L.; Lachapelle, K. 3D printing materials and their use in medical education: a review of current technology and trends for the future. *BMJ Simul. Technol. Enhanc. Learn.* **2018**, *4*, 27–40, doi:10.1136/bmjstel-2017-000234.
29. Xu, Y.; Xepapadeas, A.B.; Koos, B.; Geis-Gerstorfer, J.; Li, P.; Spintzyk, S. Effect of post-rinsing time on the mechanical strength and cytotoxicity of a 3D printed orthodontic splint material. *Dent. Mater.* **2021**, *37*, e314-e327, doi:10.1016/j.dental.2021.01.016.
30. Wulff, J.; Schweikl, H.; Rosentritt, M. Cytotoxicity of printed resin-based splint materials. *J. Dent.* **2022**, *120*, 104097, doi:10.1016/j.jdent.2022.104097.
31. Lohbauer, U.; Rahiotis, C.; Krämer, N.; Petschelt, A.; Eliades, G. The effect of different light-curing units on fatigue behavior and degree of conversion of a resin composite. *Dent. Mater.* **2005**, *21*, 608–615, doi:10.1016/j.dental.2004.07.020.
32. Barszczewska-Rybarek, I.M. A Guide through the Dental Dimethacrylate Polymer Network Structural Characterization and Interpretation of Physico-Mechanical Properties. *Materials (Basel)* **2019**, *12*, 4057, doi:10.3390/ma12244057.
33. Wulff, J.; Schmid, A.; Huber, C.; Rosentritt, M. Dynamic fatigue of 3D-printed splint materials. *J. Mech. Behav. Biomed. Mater.* **2021**, *124*, 104885, doi:10.1016/j.jmbbm.2021.104885.
34. Kim, D.; Shim, J.-S.; Lee, D.; Shin, S.-H.; Nam, N.-E.; Park, K.-H.; Shim, J.-S.; Kim, J.-E. Effects of Post-Curing Time on the Mechanical and Color Properties of Three-Dimensional Printed Crown and Bridge Materials. *Polymers* **2020**, *12*, 2762, doi:10.3390/polym12112762.
35. Rosentritt, M.; Krifka, S.; Preis, V.; Strasser, T. Dynamic fatigue of composite CAD/CAM materials. *J. Mech. Behav. Biomed. Mater.* **2019**, *98*, 311–316, doi:10.1016/j.jmbbm.2019.07.002.
36. Huang, W.; Ren, L.; Cheng, Y.; Xu, M.; Luo, W.; Zhan, D.; Sano, H.; Fu, J. Evaluation of the Color Stability, Water Sorption, and Solubility of Current Resin Composites. *Materials* **2022**, *15*, doi:10.3390/ma15196710.
37. Lohbauer, U.; Belli, R.; Ferracane, J.L. Factors involved in mechanical fatigue degradation of dental resin composites. *J. Dent. Res.* **2013**, *92*, 584–591, doi:10.1177/0022034513490734.